Measurement Characterization of Band-Pass NGD Time Domain of a 101O-Topology Passive Circuit

Xiang Zhou, Zhaoyuan Gu, Qizheng Ji, Xiaofeng Hu, Rémy Vauché, Fayrouz Haddad, Nour Mohammad Murad, Jaroslav Frnda, Wenceslas Rahajandraibe, Fayu Wan, et al.

Measurement characterization of bandpass NGD time-domain of 101O-topology passive circuit

Xiang Zhou[1], Zhaoyuan Gu[2], Qizheng Ji[3], Xiaofeng Hu,[3] Rémy Vauché[4], Fayrouz Haddad[4], Nour Mohammad Murad [5], Jaroslav Frnda[6,7], Wenceslas Rahajandraibe[4], Fayu Wan[2] and Blaise Ravelo[2]

[1] School of Mechanical Engineering, Southeast University, Nanjing, 211189, China;

[2] Nanjing University of Information Science & Technology (NUIST), Nanjing, 210044, China

[3] Army Engineering University of PLA, Shijiazhuang Campus, Shijiazhuang 050003, China ;

[4] Aix-Marseille University, CNRS, University of Toulon, IM2NP UMR7334, Marseille, France

[5] PIMENT, Network and Telecom Lab, Institut Universitaire de Technologie, University of La Reunion, Saint Pierre 97410, France

[6] Department of Quantitative Methods and Economic Informatics, Faculty of Operation and Economics of Transport and Communications, University of Zilina, 010 26 Žilina, Slovakia

[7] Department of Telecommunications, Faculty of Electrical Engineering and Computer Science, VŠB–Technical University of Ostrava, 708 00 Ostrava, Czech Republic

Email: zhouxiang@seu.edu.cn, 1540845105@qq.com, jiqizheng790308@sina.com, snowfox2270@163.com, {remy.vauche, fayrouz.haddad, wenceslas.rahajandraibe}@im2np.fr, nour.murad@univ-reunion.fr, jaroslav.frnda@fpedas.uniza.sk, fayu.wan@nuist.edu.cn,blaise.ravelo@yahoo.fr

Corresponding author e-mail: blaise.ravelo@yahoo.fr

Abstract: The negative group delay (NGD) is one of the less familiar electronic function. So far, the time-domain (TD) experimentation of NGD circuits remains a challenging task. This paper investigates an innovative TD measurement of bandpass (BP) NGD passive circuit. The topology of the considered BP NGD distributed circuit constituted by transmission line structure having 101O-geometrical shape is introduced. After the design description of the 101O-structure, the NGD response illustrates from simulation and measurement based on S-parameters. The NGD center frequency, bandwidth and value are approximately 3.6 GHz, 33 MHz and -4.9 ns, respectively. The TD measurement experimentation is based on the sine carrier modulated microwave signal generation with 50-ns duration. The 101O-NGD circuit input and output signals are plotted with innovative synchronization. It was shown from the TD simulated and measured results that the BP NGD effect induces an output envelope about 4.2-ns advanced of the test signal input.

Keywords: Bandpass (BP) negative group delay (NGD), Time-domain, Experimental technique, S-parameters, Microstrip circuit

Acknowledgements: This research work was supported in part by Jiangsu Specially Appointed Professor program and in part by the Startup Foundation for Introducing Talent of NUIST, in part by the Postgraduate Research & Practice Innovation Program of Jiangsu Province under Grant KYCX20_0966.

1. INTRODUCTION

To characterize the radio frequency (RF) and microwave communication functions, challenging time-domain (TD) tests [1-2] need to be developed. Several TD characterization techniques were deployed for familiar devices constituting the communication systems [1-2]. Nonetheless, further research effort is necessary for the TD test case of less familiar functions for the electronic design and test engineers.

Nowadays, suitable TD measurements in function of the application environments become a breakthrough for RF and microwave test research engineers. Some examples of familiar electronic devices can be cited. To characterize high-voltage channel at 5.8 GHz, an innovative measurement technique was proposed [1]. A real-time impedance characterization was introduced for radio frequency identification (RFID) communication devices [2]. For the assessment of RF exposure at 5G radio station and thermal analysis, innovative averaging time measurement techniques were developed [3-4]. With various cases of pulse signal event, transient RF measurements were used for agile supply modulator [5], over-head transmission line (TL) with integrated field sensors [6] and power detector RF circuits [7-8]. Behind the innovation in terms of measurement, the deployment of instrumentation enabling to generate appropriated RF and microwave pulse signal is an important task. Some innovative investigations were performed in [9-10] to generate short-pulse duration signals.

The pulse signal generation is also a key point for the TD measurement to analyze unfamiliar functions as the negative group delay (NGD) RF and microwave circuits. The concept of low-pass (LP) and bandpass (BP) NGD functions was initiated in [11] for the basic understanding by means of analogy with the classical filter function. The various NGD types [11] can be distinguished with the frequency band position where the group delay (GD) is negative. The NGD function meaning can be understood through its natural application to equalize the positive GD [12]. In other words, the NGD function can be expected to solve the electronic communication system imperfections due to the global delay [13] and GD undesirable effects [14-15].

Before the investigation on the innovative TD BP NGD function, it is worth to describe a brief state-of-the-art on the NGD function. The first demonstration of unfamiliar LP NGD function was performed with low frequency (LF) electronic circuits composed of lumped resistor, inductor and capacitor (RLC) passive and operational amplifier active components [16-17]. It was found that the LP NGD function is capable to propagate smoothed signals with limited bandwidth whose NGD circuit output was visualized in advance with the input [16-24]. The NGD experimentation was carried out with different types of LP NGD circuits based on operational amplifier [16-20], passive RLC-circuit [21-22] and microwave amplifier [23]. Despite this counterintuitive aspect, it is noteworthy that the NGD function does not contradict the causality [16-17]. In difference with LP NGD circuits, the BP NGD investigations were generally performed in the frequency domain with S-parameter measurements [25-29]. In [25], a BP NGD function was implemented with lumped circuit. To guarantee the possibility to operate with low attenuation loss at higher frequencies, last decade, most of BP NGD circuits as a two-port system were designed in microstrip technologies [26-29]. The circuits are implemented with fully distributed topologies without lumped elements. Despite the progressive research interest [25-32] on NGD circuits, few research works are

available on the BP NGD analysis in the TD. Thus, a lot of curious questions from RF and microwave design and test engineers remain open about the interpretation of BP NGD effect.

In the present work, to highlight this technical shadow, we decided to study the BP NGD TD analysis. An innovative TD characterization of BP NGD circuit is investigated. The prototype with NGD value and NGD bandwidth should be appropriated to the operating pulse signal. The NGD passive circuit is designed with an "101O" shape microstrip topology never being done before. The paper is organized in four different sections as follows:

- Section 2 describes the BP NGD circuit TD analysis. The different steps of the methodology will be introduced by considering the main specifications from frequency domain (FD) into the TD measurement.
- Section 3 introduces the topological diagram of the 101O distributed structure. The design of the 101O-circuit proof of concept (POC) will be described. Then, the validation will be performed with the POC BP NGD analysis. The measured NGD specifications as NGD center frequency, bandwidth and value will be defined.
- Section 4 focuses on the innovative TD BP NGD analysis of the 101O-circuit. In difference to the LP NGD characterization, the test signals must be short duration pulses modulating sine carrier coinciding with the NGD center frequency. The meaning and interpretation of BP NGD function are explained with TD results represented by the envelopes of input and output signals.
- Section 5 is the last conclusion of the paper.

2. METHODOLOGY OF THE BP NGD TD TESTING

The particularity of the BP NGD TD analysis is investigated in the present section. Acting as a microwave circuit, the NGD TD investigation remains a permanent challenge for most design and test engineers. After the methodological description, we will elaborate the BP NGD specifications from S-parameter modelling. Then, the TD analysis will be explained.

2.1 Necessity of frequency domain (FD) NGD specifications

In the area of microwave engineering, due to the high frequency measurement constraints, the BP NGD circuit model is traditionally implemented with S-parameters. Such a model can be advantageously performed by analytical approach, simulation and measurement [16-24]. Therefore, we are introducing the BP NGD analysis with the S-parameter modelling. Doing this, by denoting the angular frequency variable, ω, most of BP NGD studies depend on the measurement of GD defined by:

$$GD(\omega) = \frac{-\partial \arg\left[S_{21}^{NGD}(j\omega)\right]}{\partial \omega} \tag{1}$$

with S_{21}^{NGD} is the forward transmission coefficient and ω is the angular frequency by considering the 2-D S-matrix of the two-port system generalized in Fig. 1(a):

$$\left[S^{NGD}(j\omega)\right] = \begin{bmatrix} S_{11}^{NGD}(j\omega) & S_{12}^{NGD}(j\omega) \\ S_{21}^{NGD}(j\omega) & S_{22}^{NGD}(j\omega) \end{bmatrix}. \tag{2}$$

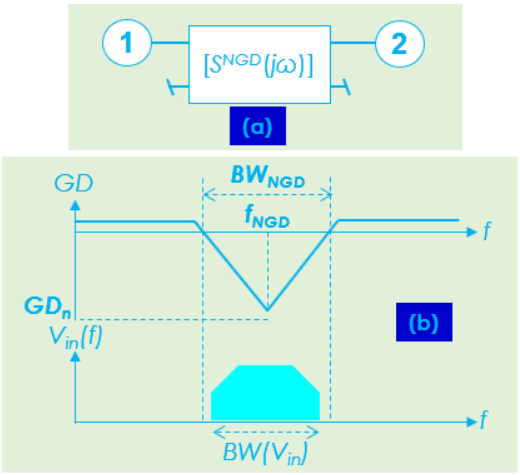

Fig. 1. (a) Two-port NGD black box and (b) spectral fundamental parameters of BP NGD responses and the expected interaction with the input spectrum.

The fundamental parameters to realize BP NGD analysis are the NGD center frequency, f_{NGD}, value, GD_n and bandwidth (BW), BW_n, which are graphically illustrated by Fig. 1(b). The BP NGD analysis golden rule is that the input signal spectrum bandwidth, $BW(V_{in})$ must be lower than the NGD bandwidth:

$$BW(V_{in}) \le BW_{NGD} \tag{3}$$

with V_{in} is the input signal. Before the TD analysis, by denoting *fft* the fast Fourier transform, the input signal spectrum:

$$V_{in}(f) = \begin{cases} 0 \quad if \quad f \notin BW(V_{in}) \\ \left| fft\left[v_{in}(t)\right] \right| \neq 0 \quad if \quad f \in BW(V_{in}) \end{cases} \tag{4}$$

must be matched to the NGD one.

2.2 General methodology of the BP NGD TD analysis

In difference to the classical RF and microwave circuit, the BP NGD circuit TD analysis must be performed with some particular rules. Because of the NGD function unfamiliarity and also the counterintuitive effect of the NGD phenomenon, some recall about the NGD specifications must be initially verified before the TD investigation. The BP NGD TD analysis can be fulfilled under the following steps:

- **Step 1**: S-parameter modelling of the NGD circuit in the expected NGD frequency band is the initial step. The modelling can be performed by analytical expression, simulations (SPICE, full wave tools, …) or measurement with vector network analyzer (VNA).
- **Step 2**: The BP NGD specifications must be identified as indicated in Fig. 1(b). Such a specification can take into account the requirement of targeted reflection and transmission coefficients:

$$\begin{cases} S_{11}^{NGD}(\omega_{NGD}) = S_{11}^{NGD}(2\pi f_{NGD}) = \left| S_{11}^{NGD}(j\omega_{NGD}) \right| \\ S_{21}^{NGD}(\omega_{NGD}) = S_{21}^{NGD}(2\pi f_{NGD}) = \left| S_{21}^{NGD}(j\omega_{NGD}) \right| \end{cases}. \tag{5}$$

- **Step 3**: The verification of equation (3) which corresponds to the input signal spectrum bandwidth to be suitable to the NGD BW as illustrated in Fig. 1(b).
- **Step 4**: Generation of the input signal, v_{in}, including the modulation by considering a sine carrier centered at the NGD center frequency, f_{NGD}.
- **Step 5**: Verification of the possibility to plot simultaneously the input and output signals, v_{in} and v_{out}, respectively.
- **Step 6**: The meaning of BP NGD function in the time-domain must correspond to the verification of the time-domain response as follows:

$$v_{out}(t) = a(t) \cdot v_{in}\left[t + \Delta t(t)\right] \approx a \cdot v_{in}(t + \Delta t) \tag{6}$$

with v_{out} is the output signal, with $a(t) \approx a$ and $\Delta t(t) = \Delta t$ are assumed to be independent to time parameter, t, when the input signal spectrum frequency band belongs to the NGD BW.

- **Step 7**: The time-delay, Δt, would be negative if the circuit behaves as a BP NGD circuit. v_{in} and v_{out} should present a good signal integrity under correlation coefficient better than:

$$corr\left[v_{in}(t), v_{out}(t)\right] \geq 95\% \tag{7}$$

with *corr* is the correlation coefficient, and the distortion can be neglected. It is noteworthy that despite this counterintuitive analytical expression, the NGD circuit respect perfectly the causality principle.

2.3 Circuit configuration for BP NGD TD analysis

The essential parameters of the NGD TD analysis are the input voltage signal, v_{in}, and the output voltage signal, v_{out}. To realize the TD analysis, we can use the touchstone model of the two-port circuit S-parameters under the transient test configured by Fig. 2. The TD analysis of BP NGD circuit must be performed in function of the NGD specifications.

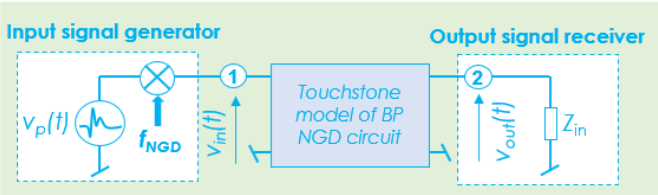

Fig. 2. Configuration of BP NGD circuit TD analysis.

The NGD characterization should be initially based on arbitrary shape pulse signal as denoted by $v_p(t)$ in Fig. 2 by assuming that the time parameter, t. In this case, the TD analysis is carried out with pulse signal modulating since carrier equal to the BP NGD center frequency:

$$v_{in}(t) = v_p(t)\sin(2\pi f_{NGD} t) \tag{8}$$

with $v_p(t)$ is the arbitrary shape pulse signal, and f_{NGD} is the NGD center frequency, t is the time parameter. Before the BP NGD TD analysis, we need to investigate on the NGD circuit POC implemented in 101O-topology in the FD.

3. BP NGD VALIDATION OF THE 101O-TOPOLOGY

This section describes BP NGD validation of the 101O-circuit topology inspired from the coupled line (CL) feedback based passive NGD cell proposed in [26-27]. The 101O microstrip prototype design, simulation and measurement validation results will be discussed.

3.1 Description of the 101O-Topology

Fig. 3 introduces the ideal diagram of the TL based 101O-circuit POC. All the constituting TLs are assumed with identical physical width, w, which was chosen to correspond to the characteristic impedance, R_0=50 Ω. The topology consists mainly of two CLs, and three pieces of TLs.

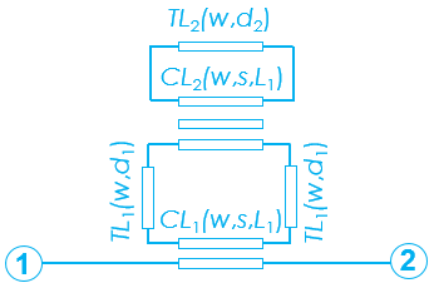

Fig. 3. Configuration of the "101O"-topology.

The four-port CL, $CL_1(w,s,L_1)$ and six-port CL, $CL_2(w,s,L_1)$ are specified by identical interspace, s, and physical length, L_1. Acting as a CL based NGD topology, the NGD center frequency be inversely proportional to this length:

$$\omega_{NGD} = \frac{c\zeta}{L_1} \tag{9}$$

with positive constant, ζ, and the vacuum light speed, c. These two CLs are interconnected by identical TLs, $TL_1(w,d_1)$ with interspace, s, and physical lengths, d_1, and d_2. Another TL, $TL_2(w,d_2)$ is interconnected to two extremities of lateral TL constituting the six-port CL, CL_2. Acting as a two-port circuit, the S-parameter and GD analyses can be performed by means of simulated and measured data corresponding to equation (1) and equation (2). The design description of the implemented 101O-circuit prototype will be explained in the following subsection.

3.2 Design of the 101O-circuit prototype

After the optimization of the physical lengths and spaces of each element of our topology, we designed the POC. Fig. 4(a) and Fig. 4(b) introduce the innovative design and photograph of the two-port 101O-circuit, respectively. It acts as a microstrip circuit implemented on Rogers 3210 substrate with specification indicated in Table 1. The constituting TLs have identical physical width, w. This microstrip circuit prototype is constituted by "101O" whose the physical sizes are addressed in Table 1.

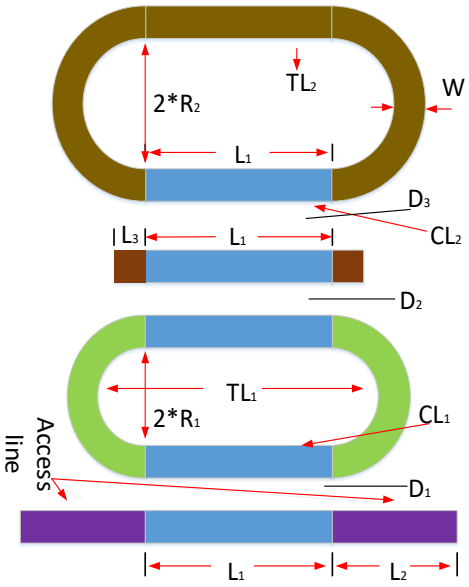

(a)

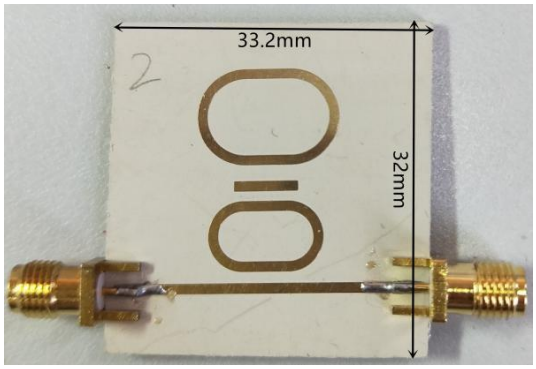

(b)

Fig. 4. (a) Design and (b) photograph of the "101O"-circuit prototype.

Components	*Description*	*Parameter*	*Value*
Substrate	Material	Rogers3210	-
	Relative permittivity	ε_r	10.2
	Loss tangent	tan(δ)	0.003
	Thickness	h	1.27 mm
Metallization conductor	Material	Copper (Cu)	-
	Thickness	t	35 µm
	Conductivity	σ	58 MS/m
CL_1	Space	D_1	1.198 mm
	Length	L_1	5.6 mm
CL_2	Space	D_2	1.071 mm
		D_3	1.748 mm
	Length	L_1	5.6 mm
		L_3	0.7 mm
TL_1	Length	R_1	2.638 mm
TL_2	Length	R_2	4.275 mm
	Width	W	1.09 mm
Access Line	Length	L_2	13.8 mm

Table 1: Microstrip circuit parameters and specifications

The coupled elements of "101O" structure are composed of different shape TLs:

- "1" element represented by the access straight line with physical length, L_1+2L_2,
- "0" element represented by the circular loop resonator with physical length, $2(L_1+\pi R_1)$,
- Other "1" element represented by the access line with physical length, L_1+2L_3,

- And last "O" element represented by the circular loop resonator with physical length, $2(L_1+\pi R_2)$.

To validate the NGD function of this prototype, S-parameter simulations with the 3-D EM commercial tool, HFSS® from Ansys® and measurement with vector network analyzer (VNA) were performed. The following subsection presents the HFSS® parametric simulation results.

3.3 Parametric analyses with respect to physical length, L_1

By curiosity, to understand the influence of length, L_1, on the NGD responses, a parametric analysis was performed. To do this, S-parameter simulations were performed from 3.4 GHz to 7.7 GHz. For each simulation, L_1 was varied from 5 mm to 6 mm. It was found that the 101O-circuit behaves a BP NGD function with two NGD center frequencies. The first NGD band results from 3.4 GHz to 3.6 GHz are mapped in Figs. 5. It can be seen in Fig. 5(a) and in Fig. 5(d) that the NGD center frequency decreases linearly from about 3.82 GHz to 3.54 GHz in the considered range of L_1.

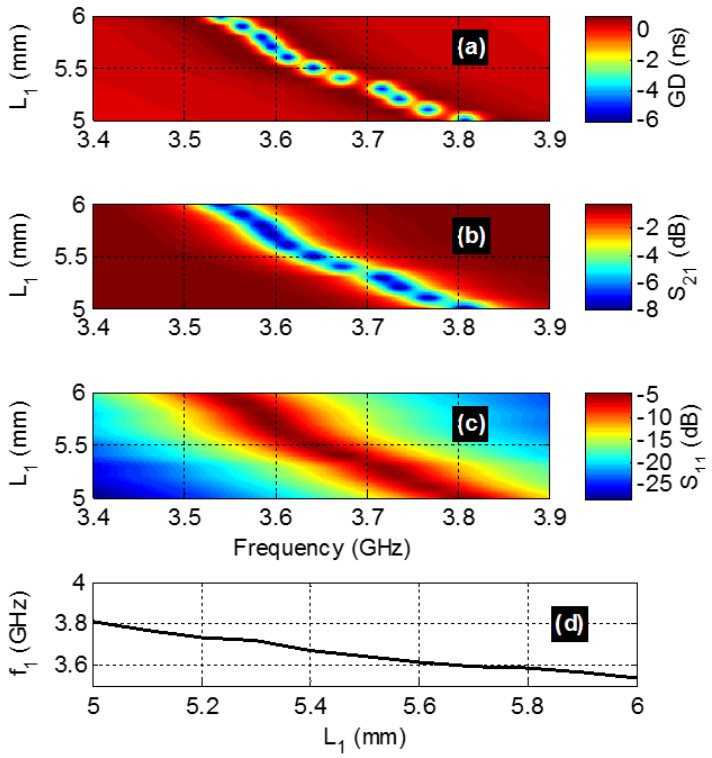

Fig. 5. Mappings of (a) *GD*, (b) S_{21}, (c) S_{11} versus (frequency, L_1) in the first BW and (d) NGD center frequency, f_1, versus L_1.

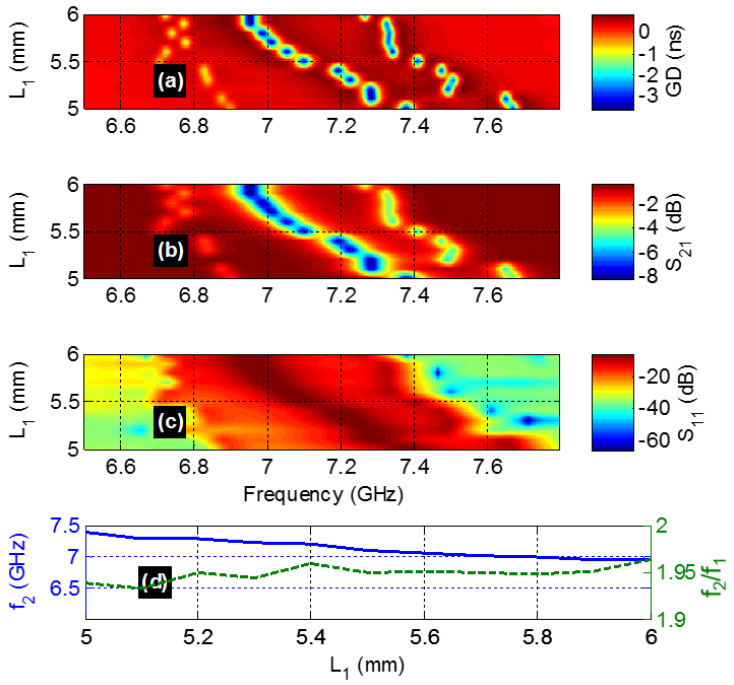

Fig. 6. Mappings of (a) *GD*, (b) S_{21}, (c) S_{11} versus (frequency, L_1) in the second BW and (d) NGD center frequency, f_2 (in blue solid line) and ratio f_2/f_1 (in green dashed line) versus L_1.

The transmission and reflection coefficient mappings are shown in Figs. 5(b) and 5(c). The transmission coefficient behavior is similar to the NGD response of Fig. 5(a) whose minimal value optimal frequency is shifting from about 3.82 GHz to 3.54 GHz. The GD, S_{21} and S_{11} in the second NGD frequency band are pointed out in Figs. 6(a), 6(b) and 6(c), respectively.

L_1 (mm)	f_1 (GHz)	$GD(f_1)$ (ns)	$S_{21}(f_1)$ (dB)	f_2 (GHz)	$GD(f_2)$ (ns)	$S_{21}(f_2)$ (dB)
5.0	3.808	-5.28	-7.77	7.379	-3.47	-7.72
5.1	3.768	-5.46	-7.77	7.284	-3.53	-7.75
5.2	3.736	-5.61	-7.86	7.281	-3.49	-7.98
5.3	3.717	-5.61	-7.89	7.226	-3.56	-8.10
5.4	3.673	-4.78	-7.30	7.193	-3.58	-8.00
5.5	3.642	-5.99	-7.94	7.099	-3.41	-7.74
5.6	3.614	-5.99	-7.98	7.052	-3.48	-7.84
5.7	3.596	-5.84	-7.85	7.011	-3.49	-7.97
5.8	3.585	-5.92	-7.94	6.985	-3.59	-8.15
5.9	3.564	-6.13	-8.00	6.952	-3.63	-8.26
6.0	3.540	-5.67	-7.84	6.952	-3.53	-8.16

Table 2: BP NGD specifications versus L_1

The NGD center frequency is decreasing from about 7.4 GHz to about 6.88 GHz as illustrated by the solid line of Fig. 6(d). Moreover, the dashed line of Fig. 6(d) confirms that second NGD center frequency, f_2, is equal to 2

times, f_1. The NGD center frequency is inversely sensitive to L_1 as forecasted in equation (3). Table 2 summarizes the influence of length, L_1, onto the BP NGD characteristics.

To verify the BP NGD behavior, comparison between simulation and measurement will be discussed in the following subsection.

3.4 Simulated and measured validations

The present validation study was performed in the same frequency band as in the previous parametric analysis. After measurement of the 101O circuit prototype displayed in Fig. 4(b), we get *GD*, S_{21} and S_{11} plotted in Figs. 7(a) to 7(f). The simulated ("Simu.") and measured ("Meas.") curves are plotted in black solid and red dashed lines. As understood in Fig. 7(a) and in Fig. 7(d), a very good correlation between the GD responses confirm that the circuit behaves as BP NGD function. The first and second NGD bands present center frequencies, around 3.6 GHz and 7.7 GHz. We can emphasize that:

$$f_2 = 2 f_1 = 2 f_{NGD} . \tag{10}$$

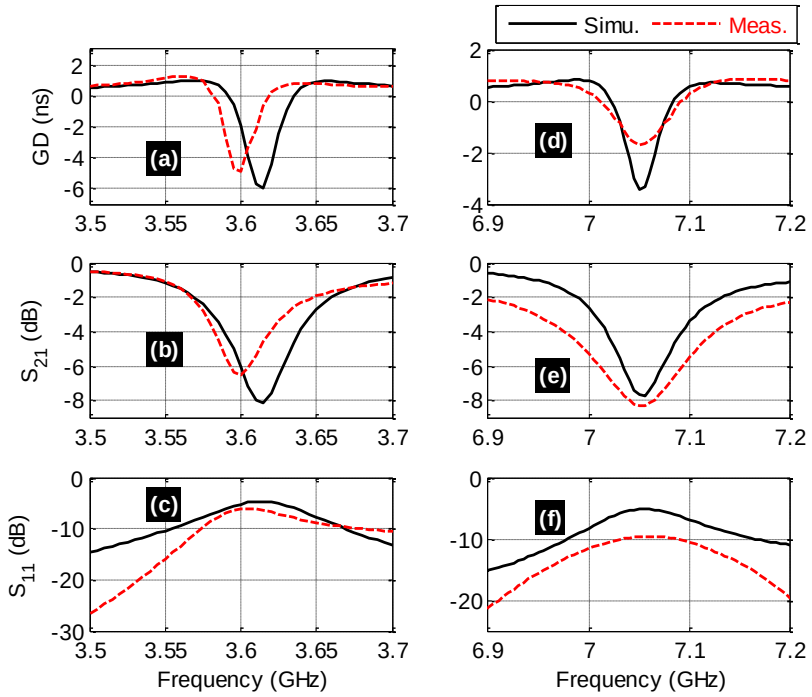

Fig. 7. Comparisons of simulated and measured in the first NGD band: (a) *GD*, (b) S_{21} and (c) S_{11} and in the second NGD band: (d) *GD*, (e) S_{21} and (f) S_{11}.

The associated BP NGD specifications are listed in Table 3. The differences between the simulated and measured results are essentially due to the imperfections of the fabricated circuit and also the full wave simulation inaccuracies. So far, open questions are wondered by the non-specialist RF and microwave design research engineers about the BP NGD function physical interpretation.

Specifications	Simulation	Measurement
Center frequency, f_1	3.615 GHz	3.6 GHz

NGD value, $GD(f_1)$	-5.97 ns	-4.913 ns
Bandwidth, BW_1	42 MHz	33 MHz
Insertion loss, $S_{21}(f_1)$	-8.18 dB	-6.55 dB
Center frequency, f_1	7.055 GHz	7.055 GHz
NGD value, $GD(f_1)$	-3.41 ns	-1.8 ns
Bandwidth, BW_2	62 MHz	80 MHz
Insertion loss, $S_{21}(f_1)$	-7.7 dB	-8.29 dB

Table 3: Simulated and measured BP NGD specifications

As a concrete interpretation of the BP NGD function focused to the first NGD band defined by the specifications ($f_{NGD}=f_1$, $BW_{NGD}=BW_1$, $GD_n=GD(f_1)$), TD investigation will be explored in the next section.

4. TD MEASUREMENT INVESTIGATION OF BP NGD CIRCUIT

So far most of BP NGD analyses were performed in the frequency domain but the interpretation of the NGD effect requires TD analysis. The TD investigation consists in the description of the experimentation concept. Then, the results of the signal behaviors interpreting the meaning of the BP NGD effect will be discussed.

4.1 TD experimental setup

Fig. 8(a) and Fig. 8(b) highlights the experimental setup of the BP NGD circuit with the 101O-prototype introduced previously in Fig. 4(b). In difference to the LP NGD TD analysis [24], the TD analysis of BP NGD requires a recovery between the input signal spectrum and the NGD bandwidth. For this reason, the input signal should be smoothed enough and must be modulated with a sine carrier. By denoting the time parameter, *t*, this TD measurement requires a generation of pulse signal modulating since carrier equal to the BP NGD center frequency:

$$v_{in}(t) = \exp\left[-A(t-t_0)^2\right]\sin(2\pi f_{NGD}t) \tag{11}$$

with the central time, t_0. The other Gaussian pulse time width parameter is defined by [30]:

$$A = \frac{\pi^2 \Delta f_{-adB}^{\ 2}}{2\ln(10^{adB/10})} \tag{12}$$

or

$$A = \frac{1}{t_1^2} \tag{13}$$

which is related to bandwidth, $\Delta f_{-adB}^{\ 2}$, defined at attenuation, *adB*. The signal plot is indicated in Fig. 7(a) with center frequency set to f_{NGD}=3.6 GHz. Then, the input and output signals must be plotted simultaneously. For this reason, we use the ultra-wide band (UWB) microwave signal generator referenced, Tektronix® AWG70001A having sampling rate equal to 50 GSps, 10 bits memory and V_{pp}=250 mV. As illustrated in Fig. 8(a), this generator is susceptible to deliver two perfectly synchronized signals from channels A and B with time shift better than 5 ps. To plot the signals, we employ the 4-channel oscilloscope referenced Agilent® DSO81204A having bandwidth 12 GHz and maximal sampling rate equal to 40 GSps and set with input impedance, $Z_{in}=R_0=50\ \Omega$. The 101O-

circuit prototype was connected to the generator and the oscilloscope through SMA connectors and 1 m-length cables. After this TD experimentation, the 101O-NGD circuit measured results are discussed in the following subsection.

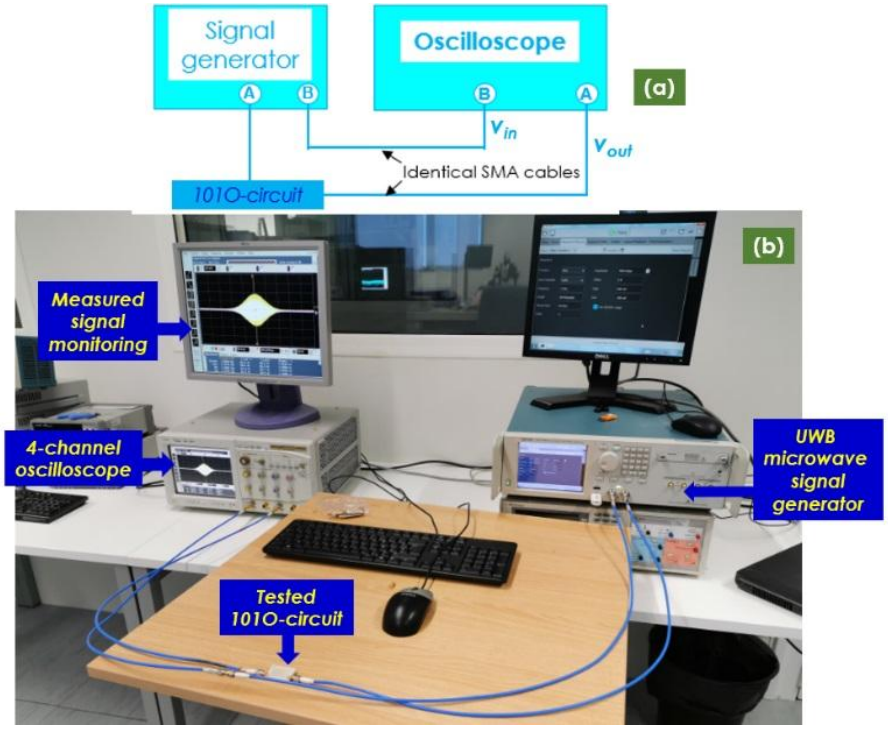

Fig. 8. (a) Illustrative diagram and (b) photograph of the TD experimental setup.

4.2 Discussion on the BP NGD circuit transient test results

The golden rule of necessary condition for the success of BP NGD operation is that the modulating pulse signal should have duration verifying a relation typically:

$$T > \frac{\xi}{BW_{NGD}} \tag{14}$$

with ξ is a positive constant depending on the fastest slop of the signal, T is the duration of the modulating pulse signal. For example, with a Gaussian pulse signal, we can take ξ=1. A Gaussian pulse defined by t_0=100 ns and t_1=25 ns, modulating, f_1=3.6 GHz sine carried was considered as the input test signal. However, input and output signals, v_{in}, and v_{out}, were plotted simultaneously in T_{max}=200 ns time range over 50 ps time step. Fig. 9(a) displays the screenshot of the NGD circuit input and output measured signals. To highlight the NGD effect, the envelopes of these signals were extracted by using signal processing algorithm implemented in MATLAB environment. Fig. 9(b) and Fig. 9(c) show that the envelopes fit perfectly with the natural transient signals. As witnessed by the envelope plots in Fig. 10(b) and the normalized plots:

$$Normalized\left[v_{in,out}(t)\right] = v_{in,out}(t) / \max\left[v_{in,out}(t)\right] \tag{15}$$

depicted in Figs. 10(c), the output signal appears with the BP NGD signature. Table 4 summarizes the TD BP NGD performance of the tested 101O-circuit. As shown in Figs. 10(d) and 10(e), the signal, v_{out}, presents leading

and trailing edges in advance of about -1.8 ns and -4.2 ns because of the BP NGD function. The input and output signal envelopes are very well correlated and verify the expectation of condition (7).

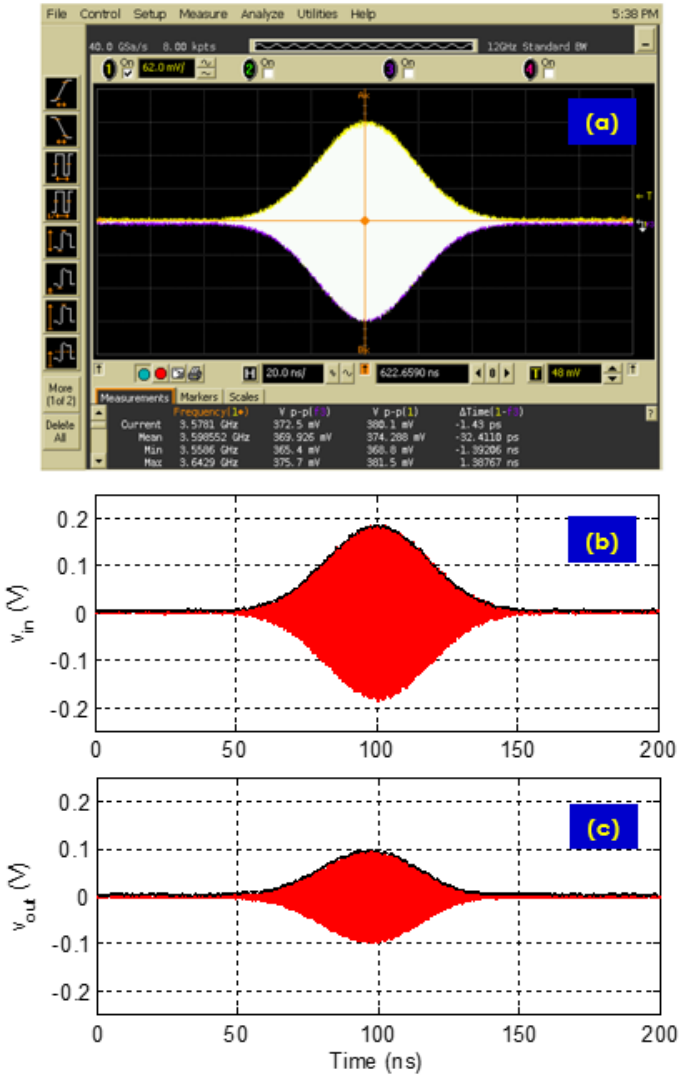

Fig. 9. Measured signals: (a) oscilloscope screen snapshot, (b) input and (c) output signals.

These TD measurement results confirm that the 101O-circuit operates as BP NGD function. It was also found during the test that if the sine carrier was shifter outside the NGD bandwidth, the output signal appears with positive delay compared to the input.

Specifications	Description	Value
Absolute rise time advance	Δt_{rise}	-1.8 ns
Relative rise time advance	$\lvert\Delta t_{rise}/t_1\rvert$	7.2 %
Absolute fall time advance	Δt_{fall}	-4.2 ns
Relative fall time advance	$\lvert\Delta t_{fall}/t_1\rvert$	16.8 %
Voltage attenuation	$a=\max(V_{out})/\max(V_{in})$	0.527
Correlation coefficient	$corr(V_{in},V_{out})$	98%

Table 4: TD NGD performance.

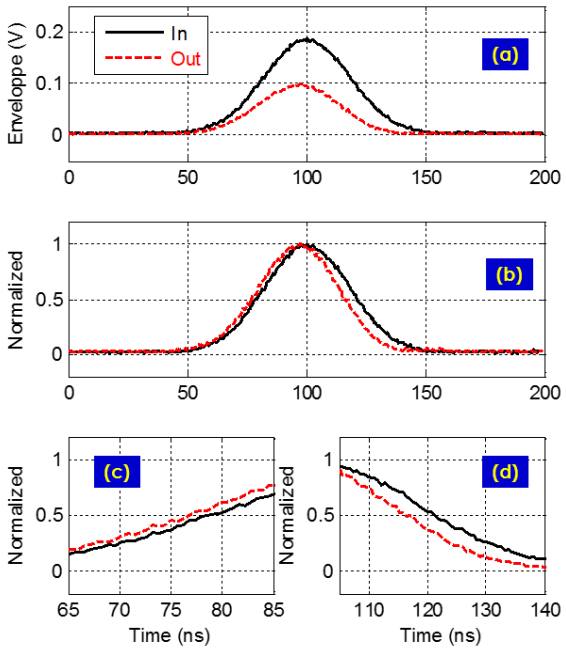

Fig. 10. (a) Natural and (b) normalized plots of input and output envelopes.

5. CONCLUSION

An innovative TD characterization of BP NGD circuit is developed. The NGD passive structure is designed with 101O-shape microstrip circuit. The BP NGD function is validated with commercial tool and measurements of S-parameters. It was found the circuit behaves as BP NGD function with center frequency of about 3.6 GHz, NGD value of about -3.6 ns and bandwidth. The TD measurement is performed with Gaussian pulse signal modulating since carrier equal to the NGD center frequency. An experimental setup guaranteeing a unrefutably synchronicity between the input and output signals is introduced. The meaning of the BP NGD aspect is validated by the output signal envelope in time-advance compared to the corresponding input.

REFERENCES

[1] C. R. Valenta, Patrick A. Graf, Matthew S. Trotter, Gregory A. Koo, Gregory D. Durgin, William G. Daly and Bradley J. Schafer, “High-Voltage-Environment Backscatter-Channel Measurements at 5.8 GHz”, IEEE Antennas and Propagation Magazine, Vol. 53, No. 4, pp. 231-240, Aug. 2011

[2] B. Couraux, T. Deleruyelle, E. Kussener and R. Vauche, “Real-Time Impedance Characterization Method for RFID-Type Backscatter Communication Devices,” IEEE Trans. Instrumentation and Measurement, vol. 67, no. 2, pp. 288-295, Feb. 2018.

[3] B. Thors, A. Furuskär, D. Colombi, and C. Törnevik, “Time-averaged realistic maximum power levels for the assessment of radio frequency exposure for 5G radio base stations using massive MIMO,” IEEE Access, vol. 5, pp. 19711-19719, 2017.

[4] K. R. Foster, et al., “Thermal Analysis of Averaging Times in Radio-Frequency Exposure Limits Above 1 GHz,” IEEE Access, Vol. 6, pp. 74536 – 74546, Nov. 2018.

[5] S. Prakash, et al. “An Agile Supply Modulator With Improved Transient Performance for Power Efficient Linear Amplifier Employing Envelope Tracking Techniques,” IEEE Trans. Power Electronics, Vol. 35, No. 4, pp. 4178-4191, Apr. 2020.

[6] Wang Hai, et al., “Transient Voltage Measurements for Overhead Transmission Lines and Substations by Metal Free and Contactless Integrated Electro-optic Field Sensors,” IEEE Trans. Industrial Electronics, Vol. 66, No. 1, pp. 571-579, 2019.

[7] A. Ildefonso, et al., “Utilizing SiGe HBT Power Detectors for Sensing Single-Event Transients in RF Circuits,” IEEE Trans. Nuclear Science, vol. 65, no. 1, pp. 239-248, Jan. 2018.

[8] Yu-Huei Lee, et al, “A DVS Embedded Power Management for High Efficiency Integrated SoC in UWB System,” IEEE Journal of solid-state, vol. 45, no. 11, pp. 2227-2238, Nov. 2010.

[9] S. Bourdel, Y. Bachelet, J. Gaubert, R. Vauche, O. Fourquin, N. Dehaese and H. Barthelemy, “A 9-pJ/Pulse 1.42-Vpp OOK CMOS UWB Pulse Generator for the 3.1–10.6-GHz FCC Band,” IEEE Trans. Microwave Theory and Techniques, vol. 58, no. 1, pp. 65-73, Jan. 2010.

[10] R. Vauche, E. Muhr, O. Fourquin, S. Bourdel, J. Gaubert, N. Dehaese, S. Meillere, H. Barthelemy and L. Ouvry, “A 100MHz PRF IR-UWB CMOS Transceiver with Pulse Shaping Capabilities and Peak Voltage Detector,” IEEE Trans. Circuits and Systems I: Regular Papers, vol. 64, no. 6, pp. 1612-1625, June 2017.

[11] B. Ravelo, “Similitude between the NGD function and filter gain behaviours,” Int. J. Circ. Theor. Appl., Vol. 42, No. 10, Oct. 2014, pp. 1016–1032.

[12] B. Ravelo, S. Lalléchère, A. Thakur, A. Saini and P. Thakur, “Theory and circuit modelling of baseband and modulated signal delay compensations with low- and band-pass NGD effects”, Int. J. Electron. Commun. (AEÜ), Ed. Elsevier, Vol. 70, No. 9, Sept. 2016, pp. 1122–1127.

[13] S.-M. Kang and H. Y. Chen, “A global delay model for domino cmos circuits with application to transistor sizing,” I. J. Circuit Theory and Applications, vol. 18, no. 3, pp. 289-306, May/June 1990.

[14] G. Groenewold, “Noise and Group Delay in Active Filters,” IEEE Trans. CAS I: Regular Papers, Vol. 54, No. 7, July 2007, pp. 1471-1480.

[15] S.-S. Myoung, B.-S. Kwon, Y.-H. Kim and J.-G. Yook, “Effect of Group Delay in RF BPF on Impulse Radio Systems,” IEICE Tran. Communications, Vol. 90, No. 12, 2007, pp. 3514-3522.

[16] M. W. Mitchell and R.Y. Chiao, “Causality and Negative Group-delays in a Simple Bandpass Amplifier,” Am. J. Phys., vol. 66, 1998, pp. 14-19.

[17] M. W. Mitchell and R. Y. Chiao, “Negative Group-delay and ‘Fronts’ in a Causal Systems: An Experiment with Very Low Frequency Bandpass Amplifiers,” Phys. Lett. A, vol. 230, Jun. 1997, pp. 133-138.

[18] T. Nakanishi, K. Sugiyama and M. Kitano, “Demonstration of Negative Group-delays in a Simple Electronic Circuit,” Am. J. Phys., vol. 70, no. 11, 2002, pp. 1117-1121.

[19] M. Kitano, T. Nakanishi and K. Sugiyama, “Negative Group-delay and Superluminal Propagation: An Electronic Circuit Approach,” IEEE J. Sel. Top. in Quantum Electron., vol. 9, no. 1, Feb. 2003, pp. 43-51.

[20] J. N. Munday and R. H. Henderson, “Superluminal Time Advance of a Complex Audio Signal,” Appl. Phys. Lett., vol. 85, July 2004, pp. 503-504.

[21] M. T. Abuelma'atti and Z. J. Khalifa, "A new CFOA-based negative group delay cascadable circuit," Analog Integrated Circuits and Signal Processing, vol. 95, pp. 351-355, Mar. 2018.

[22] W. Jian-Wu and F. Zheng-He, "Time-domain nature of group delay," Chin. Phys. B, vol. 24, no. 10 (100301, 2015, pp. 1-5.

[23] H. Mao, L. Ye and L.-G. Wang, "High fidelity of electric pulses in normal and anomalous cascaded electronic circuit systems," Results in Physics, vol. 13, no. 102348, pp. 1-9, June 2019.

[24] F. Wan, J. Wang, B. Ravelo, J. Ge, and B. Li, "Time-Domain Experimentation of NGD Active RC-Network Cell", IEEE Transactions on Circuits and Systems II: Express Briefs, Vol. 66, No. 4, Apr. 2019, pp. 562-566.

[25] K.-P. Ahn, R. Ishikawa, A. Saitou and K. Honjo, "Synthesis for Negative Group Delay Circuits Using Distributed and Second-Order RC Circuit Configurations," IEICE Trans. Electron., Vol. E92.C, No. 9, 2009, pp. 1176-1181.

[26] B. Ravelo, "Theory on Coupled Line Coupler-Based Negative Group Delay Microwave Circuit," IEEE Trans. Microwave Theory and Techniques, Vol. 64, No. 11, Nov. 2016, pp. 3604-3611.

[27] F. Wan, L. Wu, B. Ravelo, and J. Ge, "Analysis of Interconnect Line Coupled with a Radial-Stub Terminated Negative Group Delay Circuit," IEEE Trans. Electromagnetic Compatibility, Early Access, 2019, pp. 1-8.

[28] F. Wan, N. Li and B. Ravelo, "O=O Shape Low-Loss Negative Group Delay Microstrip Circuit," IEEE Trans. Circuits and Systems II: Express Briefs, vol. 67, no. 10, pp. 1795-1799, Oct. 2020.

[29] F. Wan, B. Liu, P. Thakur, A. Thakur, S. Lalléchère, W. Rahajandraibe, and B. Ravelo, "0IO-Shape PCB Trace Negative Group-Delay Analysis," IEEE Access, Vol. 8, No. 1, Dec. 2020, pp. 2169-3536.

[30] R. Vauche, S. Bourdel, N. Dehaese, J. Gaubert, O. R. Sparrow, E. Muhr and H. Barthelemy, "High efficiency UWB pulse generator for ultra-low-power applications," International Journal of Microwave and Wireless Technologies, Vol. 8, special no. 3, May 2016, pp. 495-503.

[31] A. Yuan, S. Fang, Z. Wang, H. Liu and H. Zhang, "A Novel Band-Stop Filter with Band-Pass, High-Pass, and Low-Pass Negative Group Delay Characteristics," Hindawi International Journal of Antennas and Propagation, Vol. 2021, Article ID 3207652, pp. 1-15, 2021

[32] A. Yuan, S. Fang, Z. Wang and H. Liu, "A Novel Multifunctional Negative Group Delay Circuit for Realizing Band-Pass, High-Pass and Low-Pass," Electronics, vol. 10, no. 1742, pp. 1-12, 2021